THE JOURNAL OF PHYSICAL CHEMISTRY B

Article

pubs.acs.org/JPCB

MD Simulations of the Formation of Stable Clusters in Mixtures of Alkaline Salts and Imidazolium-Based Ionic Liquids

Trinidad Méndez-Morales,[†] Jesús Carrete,[†] Silvia Bouzón-Capelo,[†] Martín Pérez-Rodríguez,[‡] Óscar Cabeza,[§] Luis J. Gallego,[†] and Luis M. Varela*[,†]

[†]Grupo de Nanomateriais e Materia Branda, Departamento de Física da Materia Condensada, Universidade de Santiago de Compostela, Campus Vida s/n E-15782, Santiago de Compostela, Spain

[‡]Departamento de Física Aplicada, Universidade de Vigo, Lagoas-Marcosende s/n E-36310, Vigo, Spain

[§]Facultade de Ciencias, Universidade da Coruña, Campus A Zapateira s/n E-15008, A Coruña, Spain

Supporting Information

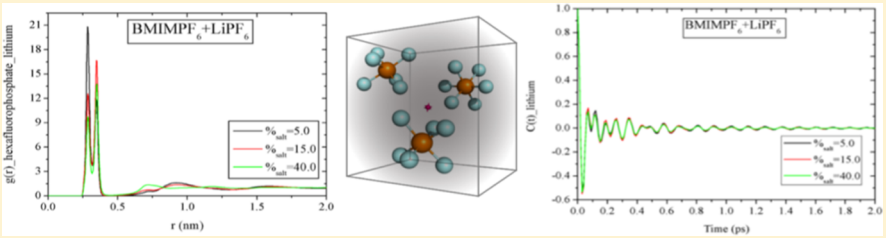

ABSTRACT: Structural and dynamical properties of room-temperature ionic liquids containing the cation 1-butyl-3-methylimidazolium ($[BMIM]^+$) and three different anions (hexafluorophosphate, $[PF_6]^-$, tetrafluoroborate, $[BF_4]^-$, and bis(trifluoromethylsulfonyl)imide, $[NTf_2]^-$) doped with several molar fractions of lithium salts with a common anion at 298.15 K and 1 atm were investigated by means of molecular dynamics simulations. The effect of the size of the salt cation was also analyzed by comparing these results with those for mixtures of $[BMIM][PF_6]$ with $NaPF_6$. Lithium/sodium solvation and ionic mobilities were analyzed via the study of radial distribution functions, coordination numbers, cage autocorrelation functions, mean-square displacements (including the analysis of both ballistic and diffusive regimes), self-diffusion coefficients of all the ionic species, velocity and current autocorrelation functions, and ionic conductivity in all the ionic liquid/salt systems. We found that lithium and sodium cations are strongly coordinated in two different positions with the anion present in the mixture. Moreover, $[Li]^+$ and $[Na]^+$ cations were found to form bonded-like, long-lived aggregates with the anions in their first solvation shell, which act as very stable kinetic entities within which a marked rattling motion of salt ions takes place. With very long MD simulation runs, this phenomenon is proved to be on the basis of the decrease of self-diffusion coefficients and ionic conductivities previously reported in experimental and computational results.

INTRODUCTION

Room-temperature ionic liquids (ILs), that is, a class of organic salts whose melting points are usually below 100 °C, have attracted considerable attention recently due to their unique and favorable properties, such as low vapor pressure, high thermal and electrochemical stability, low viscosity, high ionic conductivity, inflammability, and ability to dissolve an enormous range of organic and inorganic materials.[1−3] These properties make them very attractive "green" candidates for replacing conventional organic solvents in a variety of industrial applications[4−6] and contribute to their increasing use in various fields of chemistry: synthesis, catalysis, lubrication, thermal separation processes, purification methods, and electrochemical applications.[7−9]

Regarding electrochemical studies, the use of ILs as a new class of liquid electrolytes in lithium batteries has focused the attention of many research groups due to their nonvolatile and noncombustible natures, and it is now under investigation worldwide.[10−27] Although ILs are formed solely by ions (generally, a large organic cation, such as those based on imidazolium, pyridinium, pyrrolidinium, ammonium, or phosphonium, and an inorganic anion, such as $[PF_6]^-$, $[BF_4]^-$, $[NTf_2]^-$, etc.[28]), their use in battery electrolytes entails the addition of a lithium salt to the IL since they are not electroactive.[18] However, there is a lack of information on the solubility of lithium salts in ILs, above all, regarding the mixtures of imidazolium-based ILs with lithium salts, and only a few works presented a detailed study of the solubility of several inorganic salts in ILs up to now.[22,29−32]

With the aim of providing useful salt/IL systems that give good performance and of improving the application of ILs in lithium battery electrolytes, a detailed picture of the structural and ion transport properties of lithium salt-doped ILs is of essential importance, since they affect properties of the

Received: December 22, 2012
Revised: February 25, 2013

   dx.doi.org/10.1021/jp312669r | J. Phys. Chem. B XXXX, XXX, XXX−XXX

electrolyte (e.g., conductivity) that play a fundamental role in the performance of lithium batteries. However, the lithium cation ($[Li]^+$) solvation process and its transport mechanism in these mixtures have not been analyzed very extensively either in experimental studies or, even, by computational simulations.

In one of the experimental studies that have been published to date, Hayamizu et al.[33] measured, by using the pulsed-gradient spin−echo NMR (PGSE-NMR) method, the self-diffusion coefficients of each ion in samples of 1-ethyl-3-methylimidazolium tetrafluoroborate ($[EMIM][BF_4]$) with $LiBF_4$. They also studied the ionic conductivity, viscosity, and thermal properties up to a salt concentration of 1.5 M at various temperatures, and indicated that both the ionic conductivity and the ion self-diffusion coefficients decreased with increasing $LiBF_4$ concentration, as well as that the ions form associated structures and diffuse under the influence of the counterions in the salt/IL systems. A similar behavior for the self-diffusion coefficients was reported by Duluard et al.[34] in 2008, who analyzed the Raman spectra of 1-butyl-3-methylimidazolium bis(trifluoromethylsulfonyl)imide ($[BMIM][NTf_2]$) doped with $LiNTf_2$ for salt molar fractions $x < 0.4$. Moreover, they observed that lithium solvation is essentially due to two $[NTf_2]^-$ anions forming $[Li(NTf_2)_2]^-$ anionic clusters. This result, also obtained by Lassègues et al.,[19] was fully confirmed by Umebayashi et al.[35] by Raman spectroscopy and DFT calculations of the solvation structure of the lithium ion in 1-ethyl-3-methylimidazolium bis(trifluoromethylsulfonyl)imide ($[EMIM][NTf_2]$) and *N*-butyl-*N*-methylpyrrolidinium bis-(trifluoromethylsulfonyl)imide ($[BMPy][NTf_2]$). Also in 2008, Monteiro et al.[36] determined thermal properties, density, viscosity, ionic conductivity, and self-diffusion coefficients of mixtures of ($[BMIM][NTf_2]$) with $LiNTf_2$ at several temperatures. Their Raman spectroscopy studies indicated the formation of at least two different types of aggregates, $[BMIM]^+$ with $[NTf_2]^-$ (which they called the "weak" ones), and $[Li]^+$ with $[NTf_2]^-$ (the "strong" ones). In addition, they performed molecular dynamics (MD) simulations and showed that the average number of $[NTf_2]^-$ anions around a given $[Li]^+$ changes with salt concentration, causing a change of the structure of the mixture and provoking a reduction of diffusion coefficients of all species in the IL/salt system.

As it is usually very complicated to experimentally achieve a detailed knowledge of the behavior of lithium salt-doped ILs at the molecular level, MD simulations are an essential tool for exploring the interplay between dynamical properties and local structures in this kind of systems. One example would be the study reported by Borodin et al.,[37] in which they performed MD simulations of *N*-methyl-*N*-propylpyrrolidinium bis-(trifluoromethylsulfonyl)imide ($[MPPY][NTf_2]$) and *N*,*N*-dimethyl-pyrrolidinium bis(trifluoromethylsulfonyl)imide ($[MMPY][NTf_2]$) doped with a 0.25 molar fraction of $LiNTf_2$ at 303−500 K. They found that $[Li]^+$ cations are coordinated on average by four oxygen atoms with each oxygen atom being contributed by a different $[NTf_2]^-$ anion, that is, the formation of $[Li(NTf_2)_4]^{3-}$, and even a lithium aggregation in which two $[Li]^+$ are strongly coordinated by sharing up to three $[NTf_2]^-$ anions was observed at lower temperatures. Additionally, in a recent computational work, Niu et al.[38] performed MD simulations of 1-ethyl-2,3-dimethylimidazolium hexafluorophosphate ($[EMIM][PF_6]$) mixed with different molar ratios of $LiPF_6$ at 523.15 K and 1 bar. Their structural analysis showed that $[Li]^+$ cations are strongly coordinated by the fluorine atom of the $[PF_6]^-$ anion, and the number of hexafluorophosphates in the first solvation layer of the lithium cation is about four, and increases slightly with increasing the salt concentration. Moreover, they reported a two-dimensional radial-angular distribution study of the $[Li^+]$−P distance and Li−P−F' angle, in which they found that the $[Li]^+$−$[PF_6]^-$ complex tends to form the C_{2v} conformation (forming Li−P−F', an angle of around 45°) at low salt concentration, with C_{4v} conformation (forming Li−P−F', an angle of 0°) predominating at higher salt concentration. However, some controversy around the lifetime of these aggregates at room temperature still exists in some computational works, and the existence of long-lived stable lithium-induced anionic clusters was attributed to deficient equilibration.[37] To shed some light on this question, we report very long simulation runs to ensure the stabilization of the systems and an exhaustive study of the formation, stability, and influence on transport properties of this kind of clusters.

In this work, we present a comparison among three ILs from the imidazolium family in mixtures with lithium salts with the same anion. These ILs have the same cation: 1-butyl-3-methylimidazolium ($[BMIM]^+$), the anions being hexafluorophosphate, $[PF_6]^-$, tetrafluoroborate, $[BF_4]^-$, and bis-(trifluoromethylsulfonyl)imide, $[NTf_2]^-$, chosen by electrochemical interest. The self-diffusion coefficients of each ionic species in the binary IL/salt system were analyzed as a function of salt concentration, as well as density, radial distribution functions, coordination numbers, cage autocorrelation functions, mean-square displacements, ballistic and diffusive regimes, velocity and current autocorrelation functions, and ionic conductivity with the intent of providing an insight for understanding the structural and ion transport properties of salt-doped ILs. In addition, to our knowledge, this is the first time that the effects of the size of the cation are analyzed, reporting a brief comparison between the effects of lithium and sodium cations in mixtures of these kinds of salts with $[BMIM][PF_6]$.

The remainder of this paper is organized as follows: In the following section, we provide a detailed description of the computational procedure employed in this study. Next, we present and discuss the obtained results, and in the final section, we summarize our main conclusions.

SIMULATION DETAILS

All simulations for pure $[BMIM][BF_4]$, $[BMIM][PF_6]$, and $[BMIM][NTf_2]$, as well as their mixtures with the corresponding lithium/sodium salts ($LiBF_4$, $LiPF_6$/$NaPF_6$, and $LiNTf_2$, respectively), were performed using the Gromacs 4.5.4 package.[39] The thermodynamic state investigated was T = 298.15 K and P = 1 atm, and the salt molar percentages considered in all the systems were $\%_{salt}$ = {0, 1, 5, 10, 15, 25, and 40}, because, even though there are hardly any experimental studies concerning the solubility of lithium salts in ILs (and none related to sodium salts), some previous works have investigated mixtures of imidazolium-based ILs with lithium salts up to a salt mole fraction of x_{salt} = 0.50 (see ref 20 and references therein). The initial configurations for $\%_{salt}$ = 1, 5, and 10 were obtained by randomly inserting, respectively, 4950, 950, and 450 ionic pairs of ILs in a cubic box in order to have enough salt to yield statistically significant trajectories, whereas for the rest of the molar percentages, we considered 300 ionic pairs. The number of lithium/sodium salt molecules was calculated for each situation by considering each ionic pair as a single unit in the calculation of mole fractions.

dx.doi.org/10.1021/jp312669r | J. Phys. Chem. B XXXX, XXX, XXX−XXX

We employed the OPLS-AA force field in order to carry out the parametrization of the ions. This all-atom version of the OPLS force field, in which every hydrogen atom bonded to carbon is modeled explicitly, was developed by Jorgensen[40] for different organic liquids. The functional form of the OPLS force field is described by

$$E = \sum_i K_{b,i}[r_i - r_{0,i}]^2 + \sum_i K_{b,i}[\theta_i - \theta_{0,i}]^2 + \sum_i \left[\frac{1}{2}V_{1,i}(1 + \cos(\varphi_i)) + \frac{1}{2}V_{2,i}(1 + \cos(2\varphi_i)) + \frac{1}{2}V_{3,i}(1 + \cos(3\varphi_i)) + \frac{1}{2}V_{4,i}(1 + \cos(4\varphi_i))\right] + \sum_i \sum_{j<i} \left\{\frac{1}{4\pi\varepsilon_0}\frac{q_i q_j e^2}{r_{ij}} + 4\varepsilon_{ij}\left[\left(\frac{\sigma_{ij}}{r_{ij}}\right)^{12} - \left(\frac{\sigma_{ij}}{r_{ij}}\right)^{6}\right]\right\} \quad (1)$$

which includes intramolecular interactions, such as bond stretching, angle bending, dihedral torsion, and van der Waals and Coulombic interactions. The parameters employed in eq 1 are the force constants K, the nominal values r_0 and θ_0, the Fourier coefficients V, and the partial atomic charges q fixed on each atom center. σ_{ij} and ε_{ij} represent the Lennard-Jones radii and potential well depths, respectively, which are obtained from parameters for each type of atom by using geometric combination rules $\varepsilon_{ij} = (\varepsilon_{ii}\varepsilon_{jj})^{1/2}$ and $\sigma_{ij} = (\sigma_{ii}\sigma_{jj})^{1/2}$. The imidazolium cation was modeled by using the all-atom representation of the CH_2 and CH_3 groups in the alkyl chain, as well as that of the methyl group attached to the imidazolium ring, while lithium and sodium cations were modeled by a single site of charge +1. As for the anions, $[PF_6]^-$ was modeled as a set of seven sites with partial charges of 1.34 for the phosphorus atom and −0.39 for the fluorine atoms.[41] $[BF_4]^-$ was modeled as a set of 5 sites with partial charges of 1.176 for the boron atom and −0.544 for the fluorine atoms,[42] and $[NTf_2]^-$ was modeled as a set of 15 sites whose partial charges were reported in a previous article by Canongia-Lopes and Pádua.[43] Long-range electrostatic interactions were treated by using the particle-mesh ewald (PME)[44] method with a grid spacing of 12 nm and cubic interpolation. A cutoff distance of 1.1 nm was used for Lennard-Jones interactions, and a neighbor searching was made up to this same distance from the central ion and was updated every five simulation steps. The linear constraint solver (LINCS) algorithm[45,46] with a fourth-order expansion of the constraint coupling matrix was used to hold the bonds rigid, and long-range dispersion corrections were used for both energy and pressure.

Initial configurations were relaxed for 10^6 steps using a conjugated gradients algorithm in order to remove bad contacts resulting from the initial random configuration of ions. The maximum step size and the tolerance were set to 0.01 nm and 0.1 kJ/nm·mol, respectively. For each molar percentage of salt, the system was equilibrated for 10 ns in the isothermal−isobaric (NpT) ensemble. The results of an additional 10 ns long simulation in the isothermal−isobaric ensemble were then used for the analysis of the structure of the mixtures. The time step of the simulations was 2 fs. The temperature was controlled by using the V-rescale thermostat.[47] Cations and anions were separated in two (or three) baths with temperature coupling constants of 0.1 ps. The pressure control was set by using the Parrinello−Rahman barostat[48] with a reference pressure of 1 atm, an isothermal compressibility of 4.5×10^{-5} bar^{-1}, and a relaxation time of 0.1 ps. Moreover, we performed 10 ns long simulations in the NVE ensemble in order to remove the characteristic times of both the thermostat and the barostat, and whose starting point was taken from the equilibrating runs in the isothermal−isobaric ensemble for analyzing some of the dynamical properties of the mixtures, such as mean-square displacement, velocity and current autocorrelation functions, and self-diffusion coefficients. The energy was kept constant by using a combination of PME and a switch function for the direct-space part (PME-switch), making a search of neighbors with an automated update frequency, and increasing the number of iterations to correct for rotational lengthening in LINCS.

Each of these simulations provided us a sequence of configurations, that is, positions and instantaneous velocities of all atoms of the mixtures, which was analyzed to obtain structural and dynamical information about the aforementioned systems.

RESULTS AND DISCUSSION

Of all physical properties of interest of ILs, density is the most reliably and unambiguously determined. The values obtained from our simulations for pure ILs were $\rho_{[BMIM][PF_6]} = (1336.7 \pm 6.1)$ kg/m^3, $\rho_{[BMIM][BF_4]} = (1180.0 \pm 5.0)$ kg/m^3, and $\rho_{[BMIM][NTf_2]} = (1495.9 \pm 5.4)$ kg/m^3, which yielded a maximum deviation from available experimental results (1370, 1120, and 1430 kg/m^3, respectively)[2,49,50] of 4.6%, allowing us to be reasonably confident in our simulation model. Additionally, Figure 1 shows the concentration dependence of density for mixtures of $[BMIM][PF_6]$, $[BMIM][BF_4]$, and $[BMIM][NTf_2]$ with the corresponding lithium or sodium salt up to a molar percentage of $\%_{salt} = 40$ at 298.15 K. It can be seen that the addition of lithium salt increases the density of the mixture by about 5% at $\%_{salt} = 25$ when compared with pure ILs, in agreement with values previously reported by Borodin et al.,[37]

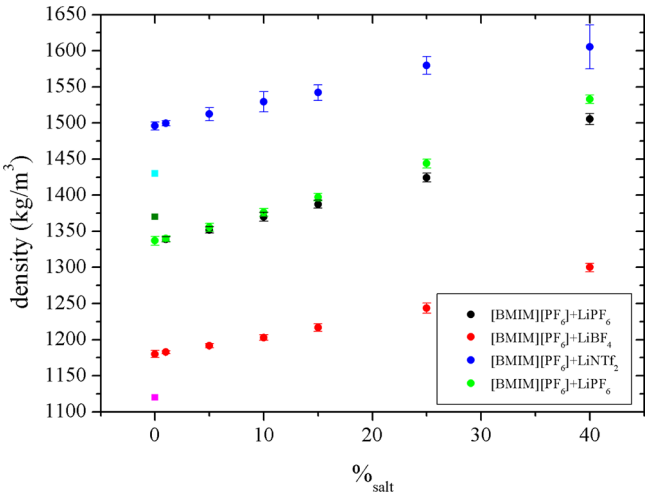

Figure 1. Simulated densities of $[BMIM][PF_6]$ (black dots), $[BMIM][BF_4]$ (red dots), and $[BMIM][NTf_2]$ (blue dots) mixed with lithium salts with a common anion as a function of the lithium salt concentration. Density of $[BMIM][PF_6]$ doped with $NaPF_6$ (green dots) is also included for the purpose of comparison. Moreover, experimental densities of the pure ILs (squares) have been included as a reference point.

dx.doi.org/10.1021/jp312669r | J. Phys. Chem. B XXXX, XXX, XXX−XXX

and about 10% at the highest molar percentage. The density of $[BMIM][PF_6]$ doped with $NaPF_6$ is included with the aim of comparing the effect of sodium cation with that of lithium in the density. As expected, replacing the lithium cation with sodium leads to an increase in the density for the same amount of salt, since lithium hexafluorophosphate is less dense than sodium hexafluorophosphate. Thus, at $\%_{salt} = 25$, an increase in the density of the mixture with sodium salt by about 8% with respect to that of the pure IL can be seen, this increase being nearly 15% at the highest amount of sodium salt.

To study the microstructure of the mixtures and gain further insight at the molecular level into the kind of aggregates that can be formed in these systems with the addition of lithium salt, we calculated radial distribution functions (RDFs)

$$g(r) = \frac{1}{\rho N}\left\langle \sum_{ij} \delta(r - r_{ij}) \right\rangle \quad (2)$$

where N is the number of particles in the system, ρ stands for its number density, i and j run over all the particles, and brackets indicate the ensemble average. It must be noted that, in the RDFs that involve the imidazolium cation, only the five atoms in the imidazole ring were considered in the calculations, and all RDFs presented in this paper were calculated using the center of mass of the molecules.

The lithium salt concentration dependence of lithium-anion RDFs is shown in Figure 2, in which we can observe that

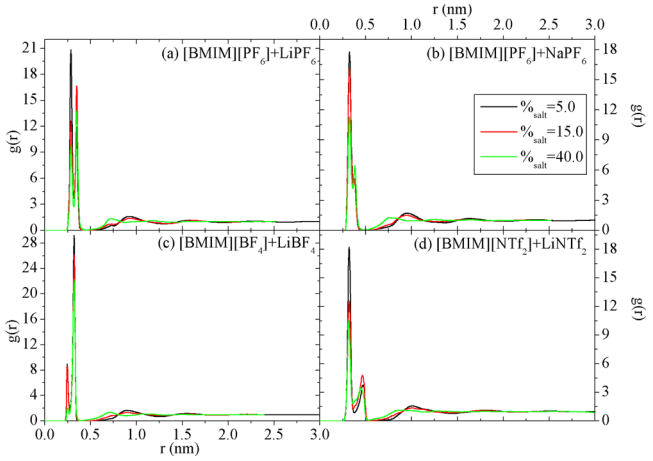

Figure 2. Salt molar percentage dependence of lithium-anion RDFs for mixtures of lithium salts with (a) $[BMIM][PF_6]$, (c) $[BMIM][BF_4]$, and (d) $[BMIM][NTf_2]$ at 298.15 K and 1 atm. Sodium-anion RDFs for $[BMIM][PF_6]$ mixed with $NaPF_6$ are also included in (b) for the purpose of comparison. For clarity, only a few of all the analyzed molar percentages are shown.

lithium molecules are strongly coordinated with the anions in all three systems, as indicated by the height of their peaks. A comparison with sodium-anion RDFs for $[BMIM][PF_6]$ mixed with $NaPF_6$ is also shown. For clarity, only a few of all the analyzed molar percentages are shown. Concerning lithium salt mixtures, if we consider that the end of the first solvation layer is placed at the position of the deepest minimum (0.4, 0.35, and 0.5 nm for $[BMIM][PF_6]$, $[BMIM][BF_4]$, and $[BMIM][NTf_2]$, respectively), a double peak can be seen within this first solvation shell in all the studied mixtures, showing that several anions coordinate with the ($[Li]^+$) cations, in agreement with previous results reported by Niu et al.[38] for $[EMIM][PF_6]$ mixed with $LiPF_6$ at 523.15 K. In mixtures in which $[PF_6]^-$ or $[NTf_2]^-$ anions are present, the first peak is sharper than the second one, whereas mixtures with $[BMIM][BF_4]$ show the opposite behavior. In addition, both peaks decrease when lithium salt is added to the mixture. If we take a look at each system separately, Figure 2a, which represents lithium-anion RDFs of $[BMIM][PF_6]$ doped with $LiPF_6$, exhibits the first peak around 0.28 nm and the second one at 0.34 nm. Those peaks correspond to the lithium cation placed between two fluorine atoms of the hexafluorophosphate anion (forming $[Li]^+-[P]^-[F]^-$, an angle of around 45°) or next to one of the fluorines (forming $[Li]^+-[P]^-[F]^-$, an angle of 0°), as represented in Figure 3a,b, respectively. These distances are in

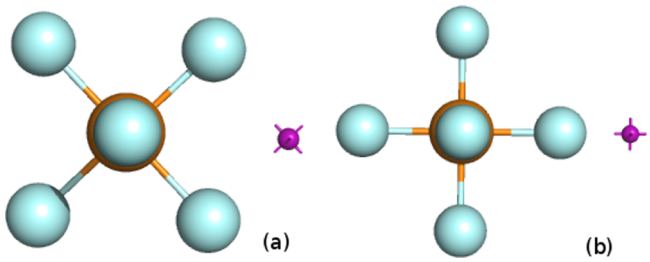

Figure 3. Representation of the two possible conformations of the lithium cation around a $[PF_6]^-$ anion in mixtures of $[BMIM][PF_6]$ with $LiPF_6$.

excellent agreement with those reported by Niu et al.[38] in their two-dimensional radial-angular distribution study. Moreover, they found that the C_{4v} conformation, which coincides with the second peak, becomes more important at higher salt concentrations, this result being consistent with the fact that, when the amount of salt present in the mixture is high, the height of the second peak becomes greater than that of the first one and, taking into account that the width of the peaks is approximately constant, height can be considered as a direct measure of the number of species in each position. On the other hand, we did not find any evidence of a tridentate coordination (C_{3v}) of lithium cations by $[PF_6]^-$, which was reported to be the most stable structure in gas phase by Xuan et al.[51] In this conformation, lithium is close to three fluorine atoms forming $[F]^-[Li]^+[F']^-$, an angle of around 73.6°, and it is placed 0.24 nm away from the central phosphorus. Figure 2c shows that the first peak of lithium-anion RDFs of mixtures of $[BMIM][BF_4]$ with $LiBF_4$ is located around 0.23 nm and the second one at 0.32 nm. This behavior is similar to the one found in mixtures of $[BMIM][PF_6]$, since the first peak corresponds to a conformation in which the lithium cation gets close to the boron atom approaching from between two of the fluorine atoms (a bidendate structure), and the second peak is consistent with a lithium cation forming an angle of 0° with a fluorine and the central boron (a monodendate mode of coordination). This second conformation is more important at all salt concentrations, as shown by the evolution of the heights of both peaks. However, in the study reported by Francisco and Williams[52] by employing ab initio quantum-chemical methods, a bidendate C_{2v} structure was predicted to be the most stable and a monodendate C_{4v} conformation was regarded as very unlikely, both structures giving $[B]^-[Li]^+$ distances in good agreement with the ones shown in Figure 2c. A tridendate C_{3v} structure with a $[B]^-[Li]^+$ distance of 0.21 nm and an intermediate stability was not found in our mixtures. Finally, Figure 2d corresponds to $[BMIM][NTf_2]$ doped with $LiNTf_2$,

dx.doi.org/10.1021/jp312669r | J. Phys. Chem. B XXXX, XXX, XXX–XXX

and it illustrates a first peak situated around 0.32 nm and a second one at 0.45 nm. This RDF is very similar to that of the lithium cation and the nitrogen atom of the anion. Therefore, it can be deduced that lithium cations are correlated to nitrogen and oxygen atoms of the anion due to their negative partial charges, since this conformation is consistent with the positions of both observed peaks. The first peak reveals a conformation in which the lithium cation is placed close to the nitrogen in an intermediate position between both sulfur atoms. The second peak is due to all the possible orientations of $[Li]^+$ around the four oxygens of the anion. This picture is in good agreement with the one reported by Borodin et al.[37] in their study of $[MMPY][NTf_2]$ mixed with $LiNTf_2$. The RDFs of $[BMIM][PF_6]$ mixed with $NaPF_6$ included in Figure 2b show, as for the mixture with lithium salt, a double peak within the first solvation layer of the central sodium cation. However, in this case, both peaks are located at slightly larger distances that those of lithium-anion RDFs, 0.32 and 0.38 nm, respectively, due to the larger size of the sodium ion. Moreover, the first peak is higher than the second one for all the studied percentages of sodium salt, showing that a conformation in which $[Na]^+$ cations are placed between two fluorine atoms of the $[PF_6]^-$ anion is always predominant in this kind of mixtures.

Packing effects on the structural conformation are shown by the evolution of the height of the two first peaks, and they can be more clearly seen in Figure 4, in which we show the

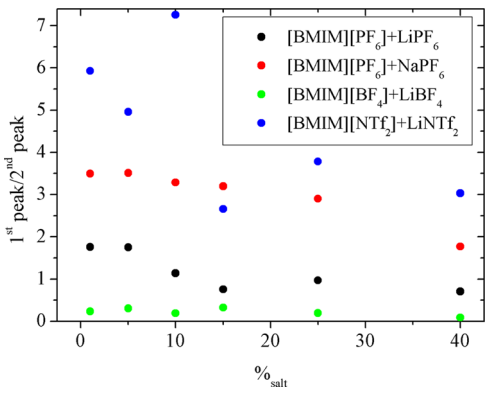

Figure 4. Salt molar percentage dependence of the relation between the height of the first two peaks for the lithium/sodium-anion RDFs of all the studied mixtures.

concentration dependence of the relation between the height of the first peak and that of the second one for the lithium/sodium-anion RDFs of all the studied mixtures. As we can observe, mixtures of $[BMIM][BF_4]$ with $LiBF_4$ are the only systems whose second peak is higher than the first one for all the analyzed molar percentages of lithium salt. On the other hand, in those mixtures of $[BMIM][NTf_2]$ and $[BMIM][PF_6]$ with $LiNTf_2$ and $NaPF_6$, respectively, the first peak is always higher than the second one, decreasing the difference between them as the amount of salt increases. Finally, $[BMIM][PF_6]$ mixed with $LiPF_6$ is the only system that shows an inversion in the height of the first two peaks with the addition of lithium salt to the mixture, since, for less than a 15% of salt, the relation between them is greater than 1 and, at higher molar percentages of salt, the relation becomes smaller than 1.

The lithium salt concentration dependence of lithium-cation RDFs for all the studied IL/salt mixtures, as well as a comparison with sodium-cation RDFs for $[BMIM][PF_6]$ mixed with $NaPF_6$, is included as part of the Supporting Information for this paper. Regarding lithium salt mixtures, in systems with $[BMIM][NTf_2]$, the first peak is a little bit displaced to higher distances than in those mixtures in which $[PF_6]^-$ or $[BF_4]^-$ anions are present, as expected due to the greater size of the $[NTf_2]^-$ anion and, therefore, of the first solvation layer. Moreover, the fact that the first peak height is lower than those of the anion-lithium RDFs and that the RDFs are quickly smoothed out implies that there is no aggregation of imidazolium cations around the lithium ions, as expected from the electrostatic interactions between cations and anions. It can be also observed that replacing lithium cations with sodium ions does not lead to a significant change in these RDFs, the most remarkable and somehow expected variation being a slightly higher first peak in the mixture with sodium salt, but with this first peak placed approximately at the same distance as the one obtained in the system doped with lithium salt.

All the studied systems exhibit an exclusion of anions after the first solvation shell, in which a layer of lithiums can be found, as we can observe looking at the first peaks in lithium−lithium RDFs, also included as Supporting Information, placed at intermediate distances between those of lithium-cation RDFs and those of lithium-anion ones. This figure also includes a comparison with sodium−sodium RDFs for $[BMIM][PF_6]$ mixed with $NaPF_6$. Thus, from the analysis of the RDFs, we can conclude that lithium/sodium cations are surrounded by a first solvation layer of anions (with which they are strongly coordinated), followed by a second shell of lithium/sodium ions and a third layer of imidazolium cations, resembling a pseudolattice structure according to the structural model on the basis of Bahe−Varela theory.[53−55] This conformation can indeed be observed in a snapshot included in Figure 5a of a few molecules in the final configuration in the simulation box of a 40% $[BMIM][PF_6]/LiPF_6$ mixture.

The above conclusions can be reinforced by evaluating the coordination numbers of ions in the mixtures. The most common way for analyzing coordination numbers in the literature is by numerical integration of the function $4\pi r^2 \rho g(r)$ up to the first minimum (ρ being the numerical density of the ionic species surrounding a lithium cation) and $g(r)$ the

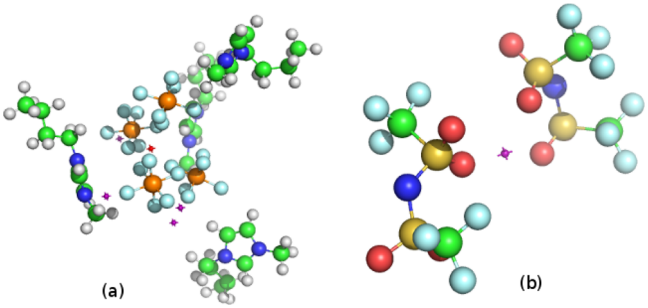

Figure 5. (a) Snapshot of a few molecules of the final configuration of a 40% $[BMIM][PF_6]/LiPF_6$ mixture, in which we can observe a central lithium cation (red) surrounded by a first layer of $[PF_6]^-$ anions, a second shell of lithium ions (violet), and a further layer of imidazolium cations. (b) Snapshot of two $[NTf_2]^-$ anions and one lithium cation of the final configuration of a mixture of $[BMIM][NTf_2]$ and a 40% of $LiNTf_2$, in which we can observe that each anion provides two oxygen atoms (red) to the first coordination shell of the lithium cation (violet).

dx.doi.org/10.1021/jp312669r | J. Phys. Chem. B XXXX, XXX, XXX−XXX

corresponding RDFs plotted in Figure 2, as well as in cation−lithium and lithium−lithium RDFs, which indicates the end of the corresponding solvation layer. The coordination number of the anions, lithium ions, and imidazolium cations in the first, second, and third coordination shells, respectively, of the $[Li]^+$ cation are shown in Table 1 for all the studied mixtures. In addition, coordination numbers corresponding to mixtures of $[BMIM][PF_6]$ with $NaPF_6$ are included, and they seem to be compatible with those of lithium ions.

Table 1. Coordination Numbers of Imidazolium Cations (Left), Anions (Center), and Lithium Ions (Right) around a Lithium Cation in Mixtures of $[BMIM][PF_6]$, $[BMIM][BF_4]$, and $[BMIM][NTf_2]$ and Lithium Salts with a Common Anion. Coordination Numbers of Imidazolium Cations (Left), Anions (Center), and Sodium Ions (Right) around a Sodium Cation of $[BMIM][PF_6]$ Mixed with $NaPF_6$ Are Also Included for the Purpose of Comparison

$[BMIM][PF_6] + [LiPF_6]$			
$\%_{salt}$	$n_{[Li]^+-[BMIM]^+}$	$n_{[Li]^+-[PF_6]^-}$	$n_{[Li]^+-[Li]^+}$
5.0	8.20	2.87	0.15
10.0	8.16	2.86	0.23
15.0	7.94	2.90	0.41
25.0	7.41	2.88	0.59
40.0	6.89	2.91	1.00
$[BMIM][PF_6] + [NaPF_6]$			
$\%_{salt}$	$n_{[Na]^+-[BMIM]^+}$	$n_{[Na]^+-[PF_6]^-}$	$n_{[Na]^+-[Na]^+}$
5.0	8.28	2.67	0.13
10.0	8.45	2.70	0.19
15.0	8.03	2.72	0.29
25.0	7.52	2.69	0.53
40.0	6.56	2.75	1.06
$[BMIM][BF_4] + [LiBF_4]$			
$\%_{salt}$	$n_{[Li]^+-[BMIM]^+}$	$n_{[Li]^+-[BF_4]^-}$	$n_{[Li]^+-[Li]^+}$
5.0	9.10	3.24	0.10
10.0	8.94	3.24	0.31
15.0	8.69	3.29	0.38
25.0	8.48	3.29	0.71
40.0	7.53	3.35	1.27
$[BMIM][NTf_2] + [LiNTf_2]$			
$\%_{salt}$	$n_{[Li]^+-[BMIM]^+}$	$n_{[Li]^+-[NTf_2]^-}$	$n_{[Li]^+-[Li]^+}$
5.0	6.55	1.91	0.04
10.0	6.12	1.84	0.13
15.0	6.39	1.96	0.26
25.0	5.49	1.90	0.42
40.0	4.47	1.71	0.59

Regarding the number of anions coordinating a $[Li]^+$ cation, it can be seen that $[BF_4]^-$ ions provide the highest value, which is approximately 3.3. In the case of $[PF_6]^-$, the value is around 3, which is in good agreement with the results reported by Niu et al.[38] In both cases, the coordination numbers slightly increase with increasing the amount of salt in the system. For the biggest anion, $[NTf_2]^-$, the coordination number reaches a value of approximately 2, which reasonably agrees with previously reported data published by Borodin et al.[37] They found that $[Li]^+$ cations are surrounded by nearly four oxygen atoms of the $[NTf_2]^-$ anion, so that our results suggest a configuration in which a single $[NTf_2]^-$ anion provides two oxygen atoms to the first coordination layer of a given lithium ion. This conformation can be observed in a snapshot included in Figure 5b of two anions around a lithium cation in the final configuration in the simulation box of $[BMIM][NTf_2]$ mixed with a 40% of $LiNTf_2$. It must be noted that Borodin et al. reported a probability for this conformation of less than 5%, whereas Duluard et al.[34] and Lassègues et al.[19,20] proposed a structure as the one that our MD simulations show of $[Li(NTf_2)_2]^-$ clusters in which the lithium is tetrahedrally coordinated to four oxygen atoms of two different anions, and as they indicated, theoretical studies suggest the formation of this bidendate structure.[56,57] As expected, the number of $[NTf_2]^-$ anions coordinated with a lithium cation is smaller than that of hexafluorophosphate or tetrafluoroborate, due to the greater size of the former. In addition, in Table 1, we can observe that the coordination numbers of imidazolium cations around a lithium atom are approximately 8 for mixtures with $[BMIM][PF_6]$ and $[BMIM][BF_4]$ and nearly 6 for those with $[BMIM][NTf_2]$. Although both cations are not strongly coordinated (as one can see in the corresponding RDF in the Supporting Information) due to the electrostatic repulsion between them, the coordination number was expected to be greater than that of any of the anions, since imidazolium cations are located in the third solvation layer of lithium ions, and due to its larger radius, this third solvation shell can accommodate a greater number of molecules than the first one. Finally, as indicated in Table 1, the number of $[Li]^+$ cations placed within the second solvation layer of lithium ions increases with lithium salt concentration in all the studied systems. The highest value, 1.3, was found in mixtures of $[BMIM][BF_4]$ at a $\%_{salt}$ = 40 of salt, whereas mixtures of $[BMIM][NTf_2]$ provided the lowest $[Li]^+-[Li]^+$ coordination number (0.6) at that same amount of salt. These results are in good agreement with the ones reported by Borodin et al.,[37] whose simulations shown that each $[Li]^+$ cation has other 0.7−0.8 lithium molecules in the second solvation layer at a salt molar percentage of $\%_{salt}$ = 25 in mixtures of $[MMPY][NTf_2]$ with $LiNTf_2$. All previous comments about mixtures of $[BMIM][PF_6]$ with $LiPF_6$ could be also extended to those with $NaPF_6$, since all the coordination numbers included in Table 1 for both cations of the salt are very similar to each other and there is no remarkable effect due to the different sizes of these ions.

To sum up, the most relevant structural features arising from our simulations are probably those concerning the position of $[Li]^+$ ions around anions, and the probable formation of bonded-like structures that could diffuse as stable kinetic entities, with all the implications this could have in what transport properties are concerned. Obviously, this hypothesis can only be tested analyzing the dynamics of $[Li]^+$ cations and anions in the bulk, what we do in the following.

Single-particle dynamics in these mixtures can be analyzed by means of the study of the center-of-mass velocity autocorrelation functions (VACFs) of their different components. The normalized VACF is calculated as

$$C(t) = \frac{\langle \vec{v}(t)\cdot\vec{v}(0)\rangle}{\langle \vec{v}(0)\cdot\vec{v}(0)\rangle} \quad (3)$$

where $\vec{v}(t)$ is the velocity of the center-of-mass of the molecule at time t and the brackets indicate the ensemble average. To the best of our knowledge, this is the first time that computational results are reported for these quantities in mixtures of ILs with lithium/sodium salts. In Figure 6, the concentration dependence of dimensionless VACFs of lithium cations are shown for

dx.doi.org/10.1021/jp312669r | J. Phys. Chem. B XXXX, XXX, XXX−XXX

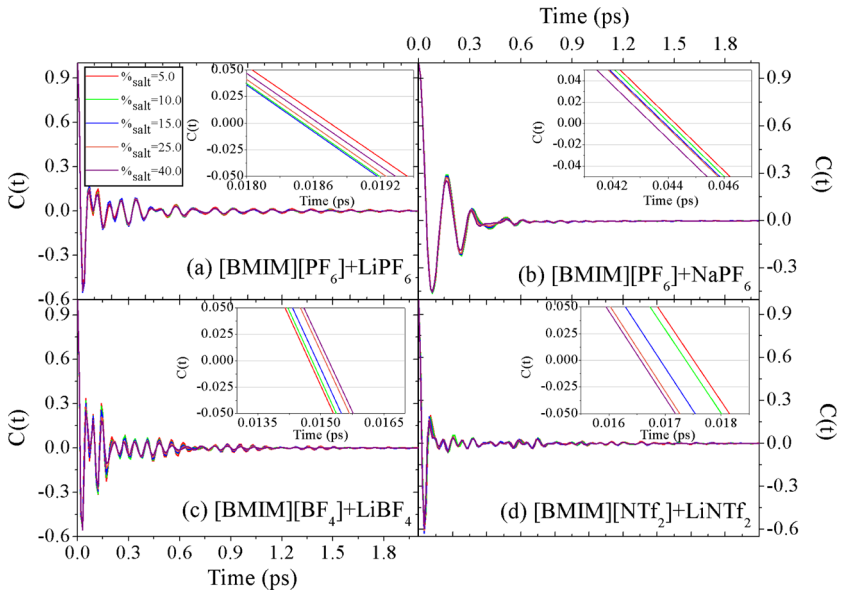

Figure 6. Concentration dependence of lithium cations VACF in mixtures with [BMIM][PF_6] (a), [BMIM][BF_4] (c), and [BMIM][NTf_2] (d). The insets show the evolution of the collision time with the amount of salt. Sodium VACFs in mixtures of [BMIM][PF_6] with $NaPF_6$ are also included in (b) for the purpose of comparison.

mixtures with [BMIM][PF_6] (a), [BMIM][BF_4] (c), and [BMIM][NTf_2] (d). This figure also includes a comparison with sodium VACFs for [BMIM][PF_6] mixed with $NaPF_6$. The insets were included in order to allow one to distinguish the evolution of the collision time, indicated by the first zero of the function, with the addition of salt to the system.

As one can see, the mean collision time shows a different trend depending on the anion that is present in the mixture. First, in cases in which hexafluorophosphate is the common anion (Figure 6a), the mean collision time increases with increasing salt concentration, except for the lowest molar percentage, for which the first zero of the function takes place at longer times. Moreover, those systems with tetrafluoroborate (Figure 6c) exhibit an increasing mean collision time as lithium salt is added to the mixture. However, the observed tendency in mixtures with bis(trifluoromethylsulfonyl)imide (Figure 6d) is exactly the opposite, since the first zero of the VACFs appears at lower times when the amount of salt increases. In addition, it must be added that, for the same amount of lithium salt, the mean collision time is somewhat longer in mixtures with [BMIM][PF_6] (around 0.0187 ps) and lower in those with [BMIM][BF_4] (around 0.015 ps), probably due to the stronger interactions between $[Li]^+$ and $[BF_4]^-$ seen in the structural analysis; the systems with [BMIM][NTf_2] being in an intermediate position (0.017 ps approximately). On the other hand, all the VACFs of the lithium cation show clear oscillations after the first collision, and this oscillatory behavior is registered up to around 1.5 ps, indicating a rattling motion of lithium ions in the "cage" of their nearest neighbors, in agreement with previous studies of lithium ions.[20,58] As expected, this rattling motion is more markedly observed the lighter the anion, probably due to the effect of the different mass ratios between the imidazolium cation and anion, since lighter anions suffer more intense oscillations in their VACFs in the presence of the same cation,[59,60] and this has an influence on lithium oscillations. In addition, a weakening of the caging effect with increasing salt concentration can be observed in mixtures with $[BF_4]^-$ anions. Moreover, the oscillations of the lithium VACFs are more rapidly weakened in this system, since the greater number of collisions of the lighter ions cancels out the correlations sooner. No evidence of long-time tails was detected in any of these mixtures. Regarding the VACFs of sodium cations, we can observe that the rattling motion of sodium ions is much less pronounced than that of lithium ions in mixtures with [BMIM][PF_6], these oscillations being completely damped after 0.8 ps, as expected due to the greater mass of sodium ions. In addition, in mixtures of [BMIM][PF_6] with sodium salts, the first zero of the function takes place at times around twice longer (0.044 ps approximately) than in mixtures with lithium salts, and the evolution of this mean collision time with the addition of sodium salt to the mixture exhibits the opposite trend of that observed for lithium salt, showing a decrease with increasing sodium salt concentration.

In addition, single-particle dynamics of the ions and the influence of the formation of aggregates on these properties were studied by analyzing, among others, the mean-square displacement (MSD), defined as

$$\mathrm{MSD}=\langle \Delta|\vec{r}(t)|^2\rangle = \frac{1}{N}\langle \sum_{i=1}^{N} |\vec{r}_i(t) - \vec{r}_i(0)|^2\rangle \quad (4)$$

where $\vec{r}(t)$ is the location of the center of mass of ion i at time t, the sum extends over all the ions present in the mixture, and brackets indicate the ensemble average. In the Supporting Information, we include an illustration (Figure S3) of the behavior of MSDs of the imidazolium cation, anion, and lithium, respectively, with increasing salt concentration in mixtures of [BMIM][PF_6]/$LiPF_6$ (a), (d), (g); [BMIM][BF_4]/$LiBF_4$ (b), (e), (h); and [BMIM][NTf_2]/$LiNTf_2$ (c), (f), (i). The results for the ions included in the systems are similar to each other, with a faster diffusion of the anions at very short times (when the expected inertial behavior takes place), and after the appearance of a crossing point at intermediate times, the MSD of the $[BMIM]^+$ cation becomes higher than that of the anion, showing a faster diffusion of the imidazolium cation at long times. After around 3 ns, the three ionic species diffuse approximately at the same rate, showing that the diffusion of

dx.doi.org/10.1021/jp312669r | J. Phys. Chem. B XXXX, XXX, XXX−XXX

Table 2. Self-Diffusion Coefficients (in 10^{-12} m^2/s) of Cation and Anion in Pure ILs Obtained by Using the Einstein Equation (6)

IL	D_{cation}^{MSD}	D_{anion}^{MSD}	$D_{cation}^{MSD-exp}$	$D_{anion}^{MSD-exp}$
[BMIM][PF_6]	1.07 ± 0.49	0.310 ± 0.021	$7^{(67)}/8^{(68)}/6.9^{(69)}$	$5^{(67)}/5.2^{(69)}$
[BMIM][BF_4]	4.32 ± 0.63	1.82 ± 0.86	$15^{(67)}/16^{(68)}/14.5^{(69)}$	$15^{(67)}/13.4^{(69)}$
[BMIM][NTf_2]	5.86 ± 0.14	4.44 ± 0.91	$25^{(67)}/32^{(68)}/27.5^{(69)}$	$20^{(67)}/21.8^{(69)}$

these ions is correlated and that they do not move separately. Furthermore, all of these three figures show that both MSDs and their slopes of all the ions decrease with increasing lithium salt concentration. We can also observe that, even though the cation is always the same, its MSD varies depending on the anion, a faster diffusion corresponds to mixtures in which $[NTf_2]^-$ is present and a slower dynamics to those with hexafluorophosphate. Moreover, the $[NTf_2]^-$ anion diffuses faster than $[PF_6]^-$ and $[BF_4]^-$, both exhibiting a similar dynamics (although faster for tetrafluoroborate), despite its greater size. Finally, the motion of the lithium cation decreases in most of the studied concentrations following the trend $[NTf_2] > [BF_4] > [PF_6]$.

In the linear representation of the MSDs, it seems that the dynamics reaches a diffusive regime after a few picoseconds, since then MSDs appear to have a linear dependence with time. However, the log−log plots of those figures, included as Supporting Information, prove that the situation is somehow more complex, and we can observe three different time scale behaviors. These three different regimes can be characterized by means of the dependence of the MSD with time, which can be measured as

$$\langle \Delta|\vec{r}(t)|^2 \rangle \propto t^{\beta} \tag{5}$$

where β describes the type of motion of the molecules of the system. The slow dynamics at intermediate times of ILs is well-known, and because of this reason, it is of fundamental importance to ensure that the ions of the ILs have reached a diffusive behavior during the simulation in order to get the correct values of long-time magnitudes, since trajectories that appear to be in the linear diffusive regime are often still subdiffusive.[61] First, the behavior of the ions at short times is ballistic, so that $\beta \simeq 2$. At the longest times, the molecules of the system exhibit linear diffusive motion after the molecules have experienced many collisions, and this Gaussian diffusion implies $\beta = 1$. Finally, at intermediate times, a subdiffusive plateau, already reported for pure ILs, characteristic of glass formers in the supercooled region, is observed.[62,63] For this non-Gaussian dynamics during the intermediate stage, related to long cage escaping time of the ions, $\beta < 1$. The log−log plots of the MSDs of lithium cations represented in graphics included in the Supporting Information show that the two transitions between the three regimes take place at similar times in all the studied systems.

To obtain a more detailed microscopic description of the single-particle dynamics of these systems, the translational diffusion coefficients can be analyzed, since this magnitude is particularly amenable for calculation with MD simulations. The self-diffusion coefficient of the ionic species i can be obtained from the long-time limit of the MSD by the well-known Einstein equation[64,65]

$$D_i^{MSD} = \frac{1}{6} \lim_{t\to\infty} \frac{d}{dt} \langle [\vec{r}_i(t) - \vec{r}_i(0)]^2 \rangle \tag{6}$$

This equation is valid only at long simulation times, when the MSD shows a linear dependence with time and a truly diffusive regime is reached, since too short MD trajectories usually provide wrongly estimated self-diffusion coefficients.[66] Particularly, in this work, we made a least-squares fit of the data between 1000 and 9000 ps in order to apply eq 6.

As a validation of the accuracy of the employed force field in what transport properties are concerned, an additional testing of the dynamical and transport properties of our model can be made by calculating the self-diffusion coefficients of pure ILs and contrasting them with available experimental and computational data. For this purpose, Table 2 shows the simulated self-diffusion coefficients of cations and anions in pure ILs obtained by using the Einstein equation (6), including their respective uncertainties, directly provided by the GROMACS package.

As can be seen, the self-diffusion coefficients calculated from MSDs are in the order of 10^{-12} m^2/s, and they underestimate the experimental values reported in the literature for pure ILs[67,68] by a factor of 4−5, which could suggest that our simulations were not long enough to let the system reach the diffusive regime and the slope of the MSD (from where the self-diffusion coefficient is estimated) is still too low. Actually, Borodin et al.[37] indicated that $[Li]^+$ motion is still subdiffusive up to 33 ns at temperatures close to room temperature. However, we performed 40 ns long simulations of pure [BMIM][PF_6] in order to check the influence of the simulation times, and we noticed no significant effect on the self-diffusion coefficients of both ionic species. In view of the obtained results, we must point out that, although the structure of the mixtures is reasonably predicted, the single-particle dynamics seems to be quite slow. This could certainly be improved using a polarizable model, as it has been discussed by Borodin et al. in previous studies.[69,70]

Moreover, although cations and anions MSDs were found to exhibit similar behavior for each IL, this route of calculation provided larger values for the cation than for the anion in all cases, despite their larger volumes and masses, an observation that shows that the diffusion of the ions is correlated, as it has been reported in previous studies.[59,67,71,72] Furthermore, self-diffusion coefficients of both cation and anion were expected to follow the trend $[NTf_2] > [BF_4] > [PF_6]$,[67] in agreement with our results.

The dependence on lithium salt molar percentage of the self-diffusion coefficients calculated from MSDs of $[BMIM]^+$, anions, and $[Li]^+$ are shown in Figure 7 in plots (a), (b), and (c), respectively. In addition, self-diffusion coefficients obtained from the slope of MSDs of the imidazolium cation, hexafluorophosphate, and sodium in systems with $NaPF_6$ doping [BMIM][PF_6] are included. In agreement with previous studies of mixtures of ILs with lithium salts,[18,26,33,34,36,38] the motion of the ions is sensitive to the lithium salt concentration, and in binary systems, the increase in the amount of salt causes a slight decrease of the self-diffusion coefficients of all the ions, although, in mixtures in which the hexafluorophosphate anion is present, this trend is not as clear as in those mixtures with the

dx.doi.org/10.1021/jp312669r | J. Phys. Chem. B XXXX, XXX, XXX−XXX

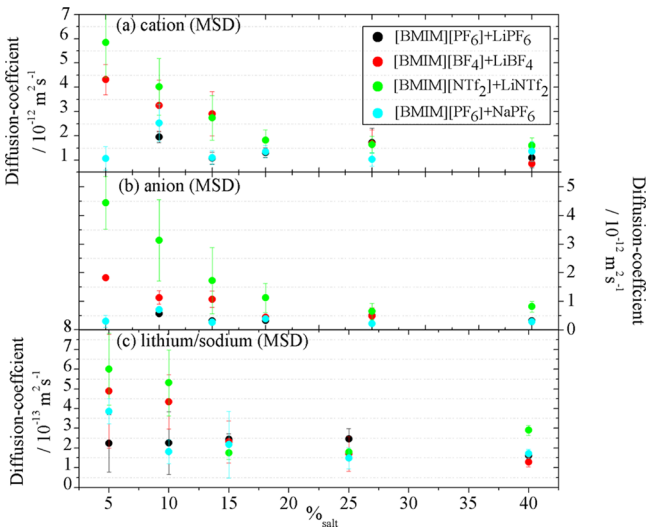

Figure 7. Concentration dependence of the self-diffusion coefficients of cation (a), anions (b), and lithium (c), calculated by using the Einstein equation (6). Self-diffusion coefficients of imidazolium cation (a), hexafluorophosphate (b), and sodium (c) obtained from MSDs for [BMIM][PF_6] doped with $NaPF_6$ are also included with the aim of comparison.

other two anions. Moreover, it can be seen that the smallest ion, $[Li]^+$, is always the slowest species, with the imidazolium cation being the fastest and the anions occupying intermediate positions, as reported in the literature.[33,34,36,38] This slower motion of the lightest ionic species was also found in mixtures of ILs with aluminum salts,[73] and it was reported that their greater equivalent surface charge density reduces drastically the mobility of these ions and forces them to remain in almost fixed equilibrium positions. On the other hand, self-diffusion coefficients for the lithium cation was found to be around 1 order of magnitude lower than expected, since, as for cations and anions, lithium coefficients are also in the order of 10^{-11}–10^{-12} m^2/s, but with lower coefficients.[33,34,36] It can be observed that self-diffusion coefficients of the imidazolium cation, hexafluorophosphate, and sodium in the [BMIM][PF_6]/$NaPF_6$ systems are very close to those of the lithium salt mixtures at the same amount of salt, but slightly lower in the case of the sodium ion, probably due to the effect of the different size of the $[Na]^+$ cation. From the Stokes–Einstein equation

$$D_i = \frac{k_B T}{c\pi\eta r_i} \tag{7}$$

where T is the temperature of the mixture, c is a constant, η is the viscosity of the system, and r_i is the effective hydrodynamic radius of molecule i. From this relation, we could conclude that the greater the size of the ion, the slower it is. However, as we said for the self-diffusion coefficients obtained from the MSD curves, this is not the trend obtained in previous experimental studies. The existence of small clusters involving $[Li]^+/[Na]^+$ cations and anions is strongly suggested from our structural analysis, as it has also been observed in previous publications.[19,37,38,74] Thus, we conclude that both lithium and sodium form kinetic entities with its surrounding anions, thus, reducing their mobilities. For example, Duluard et al.[34] estimated the diffusion coefficients of the free $[NTf_2]^-$ anions and of those involved in anionic $[Li(NTf_2)_2]^-$ clusters, and they also found that the value of the latter was similar to that of the lithium cation. The first solvation shell of the lithium/sodium ions is expected to be dynamically broken and formed,[37,38] with a transport mechanism in which lithium/sodium moves from one anion to another, but with a quite low hopping rate (of $[Li]^+/[Na]^+$ cation) and strong aggregation. Hence, our study of VACFs and MSDs suggests a picture in which lithium ions are moving inside the cages formed by their nearest neighbors suffering many collisions with the anions around them before reaching a subdiffusive motion, since the first collision of lithium cations takes place at much shorter times than that of the end of the ballistic region (around 0.017 and 1 ps,

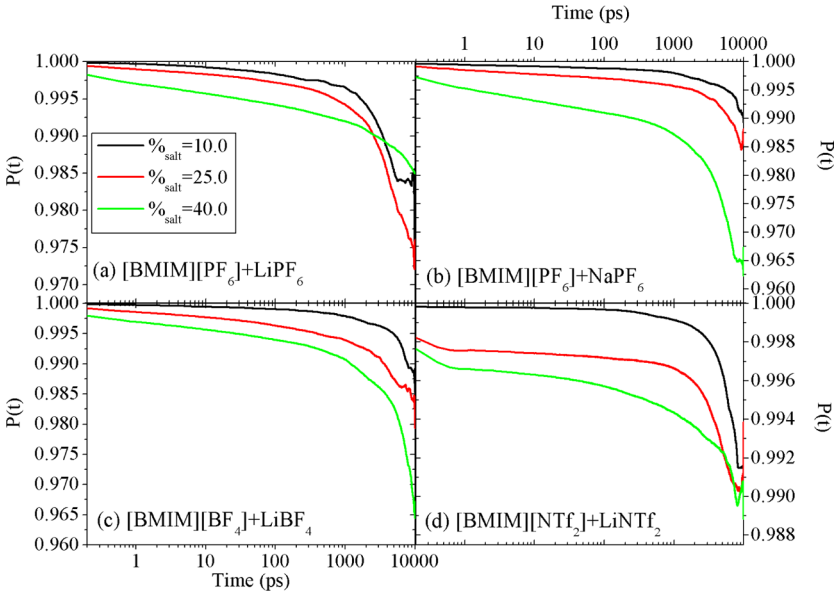

Figure 8. Concentration dependence of CaACFs of anions within the first solvation layer of lithium cations in mixtures with [BMIM][PF_6] (a), [BMIM][BF_4] (c), and [BMIM][NTf_2] (d). CaACFs of $[PF_6]^-$ anions coordinating sodium cations in mixtures of [BMIM][PF_6] with $NaPF_6$ are also included in (b) for the purpose of comparison.

dx.doi.org/10.1021/jp312669r | J. Phys. Chem. B XXXX, XXX, XXX–XXX

respectively). This is also confirmed by the strong correlation of the velocity of $[Li]^+$ cations with their initial velocity, as indicated by the long-lived oscillations shown in the VACFs, and in agreement with the effect of the mass ratio between the lighter lithium and the heavier anions in an elastic collision between them. This is not the behavior found in mixtures with water[75] or alcohols,[76] for which collision and ballistic times were very similar to each other. Water molecules seem to have a few collisions with other water molecules surrounding them before reaching the subdiffusive regime, whereas alcohol molecules have more similar masses to their coordinating anions so their VACFs do not show marked rattling motion regions. Once again, these deeds suggest the formation of stable kinetic aggregates induced by lithium cations.

To obtain additional insight of the dynamics of lithium and sodium cations and their coordinating anions, we analyzed the lifetime of these structures by calculating a cage autocorrelation function (CaACF) defined as[37,38]

$$P(t) = \frac{\langle H_{ij}(t)H_{ij}(0)\rangle}{\langle H_{ij}(0)H_{ij}(0)\rangle} \tag{8}$$

where $H_{ij}(t)$ takes the value of 1 if $[Li]^+/[Na]^+$ cations, i, and the center of mass of their surrounding anions, j, are closer than the position of the first minimum of the lithium/sodium-anion RDFs at time t, and zero, otherwise. The brackets $\langle\rangle$ indicate the average over all time origins. In Figure 8, the concentration dependence of CaACFs of the anionic clusters formed by lithium cations and anions in their first coordination shell is shown for mixtures of lithium salt with $[BMIM][PF_6]$ (a), $[BMIM][BF_4]$ (c), and $[BMIM][NTf_2]$ (d). This figure also includes a comparison with CaACFs of the complexes present in $[BMIM][PF_6]$ mixed with $NaPF_6$.

It can be observed that the decay of the CaACFs in mixtures with the lowest concentrations is slower than in those with the highest amount of salt, showing that the increasing of lithium salt in the mixture leads to the formation of less rigid structures, which is due to the fact that each lithium added to the mixture needs 2−3 coordinated anions. This tendency is compatible with the fact that the ionic mobility decreases with the amount of salt in the mixture, since a slower motion of the whole aggregate, which seems to be the entity that reaches the diffusive regime, does not imply a longer stability of that cluster. It can be also noted that the stability of the complexes in those mixtures of $[BMIM][PF_6]$ with $LiPF_6$ is less sensitive to salt amount variations than in the rest of the systems, since the curves of CaCAFs are more similar to each other. The most remarkable aspect seen in Figure 8 is the strong memory effect and the very large association−dissociation characteristic times of $[Li(Anion)_n]^{n-1}$ aggregates, which is shown by the slight decay of all the CaACFs (after 10 ns, none of the CaACFs decayed more than 5%). Borodin et al.[37] found a similar result for $[MPPY][NTf_2]$ and $[MMPY][NTf_2]$ doped with a 0.25 molar fraction of $LiNTf_2$ at 303−333 K, but they attributed this result to the fact that their systems were not well-equilibrated. However, we must point out that we ensured the equilibration of our mixtures by performing two 50 ns long simulations, one in the NVE ensemble and the other one in the NpT ensemble, both also giving a decay of less than 5%. In addition, we further proved the resilience of these structures, verifying that the anions surrounding a given $[Li]^+$ in every time frame of the simulation run are always the same. Residence times of tens and even hundreds of nanoseconds of lithium ions inside the cages formed by their nearest neighbors were previously reported by Borodin et al.[77] in simulations of amorphous dilithium ethylene dicarbonate (Li_2EDC) and lithium methyl carbonate (LiMC) at temperatures from 393 to 600 K. On the other hand, the relatively fast decay of $P(t)$ found by Niu et al.[38] in $[EMIM][PF_6]$ mixed with $LiPF_6$ can be due to the high temperature at which they performed the runs, 523.15 K, which is consistent with the results reported by Borodin et al.[37] at 393 K and shows the great effect of the temperature on this magnitude. All previous comments can be referred to those mixtures of $[BMIM][PF_6]$ with $NaPF_6$, since CaACFs of systems with sodium salt do not show significative differences compared to the ones with lithium beyond a slightly slower decay.

From this analysis, we conclude that the first solvation shell of lithium/sodium cations is very stable, leading to the formation of strong and long-lived $[Li(Anion)_n]^{n-1}$ anionic clusters. Thus, even though, in our single-particle dynamics analysis, the results from MSDs and VACFs seemed to be somewhat contradictory, it has been shown that they lead to a picture in which $[Li]^+$ and $[Na]^+$ diffuse altogether with their surrounding anions as a stable kinetic entity; meanwhile, they suffer a rattling motion inside those clusters, in agreement with several previously reported experimental studies.[18,20,33,34]

Further information about the dynamics of the system can be obtained by studying another interesting magnitude, the current autocorrelation function (CACF), which can be calculated from NVE simulations as

$$J(t) = \frac{\langle \vec{j}(t)\cdot\vec{j}(0)\rangle}{\langle \vec{j}(0)\cdot\vec{j}(0)\rangle} \tag{9}$$

where the electrical current, $\vec{j}(t)$, is given by

$$\vec{j}(t) = \sum_{i=1}^{N} q_i\vec{v}_i(t) \tag{10}$$

and q_i represents the charge of ion i and $\vec{v}_i$ stands for the velocity of the center of mass of that ion. The CACF can be also defined as the sum of two contributions, the self- and the cross-term[63,78]

$$J(t) = C(t) + \Delta(t) \tag{11}$$

the self-term, $C(t)$, being the total VACF of the system and the cross-term, $\Delta(t)$, the deviation from the ideal Nernst−Einstein relation[79]

$$\sigma_{NE} = \frac{e^2}{Vk_BT}\sum_{i=1}^{N} n_iD_i \tag{12}$$

where e is the electron charge, V is the volume of the system, T stands for the temperature, n_i represents the total number of ions of species i, and D_i is its self-diffusion coefficient. If the overall effect of cross-correlations was negligible, the normalized velocity and current autocorrelation functions would be expected to coincide. This is the assumption made in eq 12, and therefore, the decisive part missing in this relation are the cross-correlations of the single particle velocities, that is, $\langle\vec{v}_i(t)\cdot\vec{v}_i(t)\rangle$ (for $i \neq j$), of which a pair of ions with opposite charges would contribute to diffusion, but not to conductivity, leading to a significant decrease of this magnitude.

The evolution for a few molar percentages of lithium salts of the normalized total VACFs (red), the normalized CACFs (green), and the difference between them, $\Delta(t)$ (blue), are

dx.doi.org/10.1021/jp312669r | J. Phys. Chem. B XXXX, XXX, XXX−XXX

included in the Supporting Information (Figure S5), in order to analyze the relevance of cross-correlations in [BMIM][PF_6]/$LiPF_6$ (a), (e), (i); [BMIM][PF_6]/$NaPF_6$ (b), (f), (j); [BMIM][BF_4]/$LiBF_4$ (c), (g), (k); and [BMIM][NTf_2]/$LiNTf_2$ (d), (h), (l) mixtures. The importance of the correlations among ions can be clearly observed in the difference between the total VACFs and the CACFs registered, above all, at short times. The x-intercept and decay times for the CACFs are shorter than those of the VACFs, providing a negative value of the $\Delta(t)$ terms for all the studied molar percentages, which shows that neutral pairs of ions of opposite charge tend to diffuse together and do not contribute to charge transport.[63,78,80] In addition, in all the systems, $\Delta(t)$ reaches positive values, which indicates that the correlation between ions with charges of the same sign can also have significant effects. In our case, both effects nearly cancel each other and cross-correlations can be considered as negligible, leading to a good agreement of the conductivity calculated by employing the Nernst−Einstein equation (12) and that obtained by means of the Green−Kubo relation

$$\sigma_{GK} = \frac{1}{3k_B TV}\int_0^\infty \langle \vec{j}(t)\cdot\vec{j}(0)\rangle \, dt \tag{13}$$

In Table 3, we include the ionic conductivities obtained from the Nernst−Einstein equation (12) using self-diffusion coefficients calculated by employing MSDs reported in Figure 7 for the three pure ILs and their mixtures with lithium salts. It must be noted that, due to the fact that $[Li]^+$ cations are coordinated with the same anions for very long times, each lithium can be considered as neutralized by one of the anions in its solvation shell, and because of this reason, we do not consider the contribution of these neutral pairs to the Nernst−Einstein relation in order to calculate the ionic conductivity. The results of the ionic conductivity for the pure systems are only slightly underestimated by a factor of 3 for pure [BMIM][BF_4] and [BMIM][NTf_2], since the expected values were about 3.5 and 3.9 mS/cm, respectively.[2,81] In the case of pure [BMIM][PF_6], the experimental conductivity is approximately 1.5 mS/cm, which leads to an underestimation of our simulated value by around a factor of 6.[2,82] These underestimations of the ionic conductivities are associated with the smaller values of the self-diffusion coefficients of MSDs, but the trend of the conductivity [BMIM][NTf_2] > [BMIM][BF_4] > [BMIM][PF_6] was obtained. On the other hand, it was found that the Nernst−Einstein ionic conductivity calculated by using self-diffusion coefficients from MSDs decreases with increasing the amount of salt added to mixtures, which was already reported in some previous studies,[10,33] and it is the expected trend for mixtures of ILs with lithium salts with a common anion,[29] since the increase in the viscosity with increasing salt concentration leads to a lower mobility of the carrier ions. However, the decrease obtained is not as pronounced as the one reported by Monteiro et al.,[36] since they found an ionic conductivity of 0.06 mS/cm in mixtures of [BMIM][NTf_2] with a 40% of $LiNTf_2$ at room temperature. In addition, mixtures with lithium hexafluorophosphate show an unexpected increase in the conductivity at the higher amounts of salt related to the behavior of the self-diffusion coefficients in these mixtures, for which we have not seen a clear decrease with increasing lithium salt concentration. These fluctuations of the electrical conductivity could be associated with concentration fluctuations in a metastable supersaturated phase, but this possibility demands further analysis.

Table 3. Ionic Conductivity (in mS/cm) of Pure ILs ([BMIM][PF_6], [BMIM][BF_4], and [BMIM][NTf_2]) and their Mixtures with Lithium Salts with a Common Anion Obtained from the Nernst−Einstein Equation (12) Using Self-Diffusion Coefficients Calculated by Employing MSDs Reported in Figure 7

[BMIM][PF_6] + [$LiPF_6$]	
$\%_{salt}$	σ_{NE}^{MSD}
0.0	0.242
5.0	0.197
10.0	0.114
15.0	0.112
25.0	0.162
40.0	0.206
[BMIM][BF_4] + [$LiBF_4$]	
$\%_{salt}$	σ_{NE}^{MSD}
0.0	1.200
5.0	0.849
10.0	0.760
15.0	0.340
25.0	0.389
40.0	0.195
[BMIM][NTf_2] + [$LiNTf_2$]	
$\%_{salt}$	σ_{NE}^{MSD}
0.0	1.372
5.0	0.933
10.0	0.567
15.0	0.363
25.0	0.207
40.0	0.177

CONCLUSIONS

We performed MD simulations of three imidazolium-based ILs, [BMIM][PF_6], [BMIM][BF_4], and [BMIM][NTf_2], mixed with lithium salts with a common anion, and we investigated several structural and dynamical properties of the systems at T = 298.15 K and P = 1 atm. We also included mixtures of [BMIM][PF_6] with $NaPF_6$ for the purpose of comparison, in order to observe the effect of the size of the monatomic cation in the analyzed properties. Particularly, lithium/sodium solvation and ionic mobilities were studied via the analysis of radial distribution functions, coordination numbers, mean-square displacements, cage autocorrelation functions, self-diffusion coefficients of all the ionic species, velocity and current autocorrelation functions, and ionic conductivity in all the ionic liquid/salt systems.

With the aim of checking the accuracy of the employed force field, we calculated the densities of the three pure ILs and compared them to experimental data. Our simulated densities showed a maximum deviation from available experimental values of 4.6%. Additionally, the densities of the mixtures were found to decrease with increasing lithium salt concentration, in good agreement with the experimental results available in the literature.

The analysis of the RDFs of the mixtures showed that lithium/sodium cations are surrounded by a first solvation layer of anions (with which they have stronger correlations), followed by a second shell of lithium/sodium molecules and

dx.doi.org/10.1021/jp312669r | J. Phys. Chem. B XXXX, XXX, XXX−XXX

a third layer of imidazolium cations. In the three systems, the first solvation layer of $[Li]^+/[Na]^+$ is occupied by anions in two different possible conformations that are sensitive to the amount of salt present in the mixture, as shown by the presence and the evolution of the two sharp peaks in the lithium/sodium-anion RDFs. The study of the coordination numbers provided a central $[Li]^+$ cation surrounded by about 3, 3.3, and 2 anions for mixtures with hexafluorophosphate, tetrafluoroborate, and bis(trifluoromethylsulfonyl)imide, respectively, this value being slightly increased for increasing lithium salt concentration. Moreover, the $[Na]^+$ cation was found to have nearly three hexafluorophosphates around it. All of these facts suggest the formation of $[Li/Na(Anion)_n]^{n-1}$ stable kinetic entities, which was further confirmed by means of the analysis of lithium and sodium single-particle dynamics.

VACFs of lithium and sodium cations were also reported, and they revealed an oscillatory behavior up to around 1.5 and 0.8 ps, respectively, indicating a remarkable rattling motion of lithium and sodium ions in the "cage" of their nearest neighbors. This rattling motion was more markedly observed for mixtures with tetrafluoroborate anions, and an enhancement of the caging effect with decreasing salt concentration can also be seen is this system. In addition, the analysis of the salt cation CaCAF proved this structure to be extraordinarily resilient, since it was seen to survive during tens of nanoseconds, providing a further confirmation of the occurrence and stability of $[Li/Na(Anion)_n]^{n-1}$ clusters in the bulk mixture that can be considered to act as real kinetic entities. On the other hand, the self-diffusion coefficients were calculated from the Einstein relation, predicting a decrease of the mobility of all the ionic species with increasing salt concentration, in agreement with previously reported experimental results and as a possible consecuence of the formation of the clusters. However, although the self-diffusion coefficients obtained from the slope of MSDs provided a trend of the ionic motion of $[BMIM]^+ > [anion]^- > [Li]^+$, they were slightly underestimated for our analyzed simulation times. The analysis of CACFs and cross-correlations showed that effects of correlations between ions with charges of the same and opposite sign cancel each other, causing a negligible contribution of cross-correlations to the Nernst−Einstein equation. Thus, the ionic conductivity at room temperature was reported for lithium/sodium salts mixed with imidazolium-based ILs for the first time up to our knowledge, using the Nernst−Einstein relation combined with the self-diffusion coefficients from the slope of the MSDs. This method provided slightly underestimated values of the ionic conductivity, and it showed that this magnitude decreases with increasing lithium salt concentrations, in accordance to experimental observations and in line with the experimental fact that an increase in viscosity slows down the ionic mobility of the components of the mixture.

In summary, all the presently reported structural and dynamic evidence can only be understood if long-lived, stable $[Li/Na(Anion)_n]^{n-1}$ clusters are formed in the bulk solution, in which the salt cation is diffusing in a bonded-like state with the anions of its first coordination shell giving rise to stable kinetic entities whose lifetimes span over tens of nanoseconds.

■ ASSOCIATED CONTENT

Supporting Information

Figures equivalent to Figure 2, for cation−lithium and lithium−lithium RDFs, tme dependence of the MSDs and their log−log plot, and total velocity and current autocorrelation functions and the cross-terms. This material is available free of charge via the Internet at http://pubs.acs.org.

■ AUTHOR INFORMATION

Corresponding Author

*E-mail: luismiguel.varela@usc.es.

Notes

The authors declare no competing financial interest.

■ ACKNOWLEDGMENTS

The authors gratefully acknowledge Prof. R. M. Lynden-Bell for many fruitful discussions. The authors wish to thank Xunta de Galicia for financial support through the research projects of references 10-PXI-103-294 PR and 10-PXIB-206-294 PR. Moreover, this work was funded by the Spanish Ministry of Science and Innovation (Grant No. FIS2012-33126). All of these research projects are partially supported by FEDER. T.M.-M. thanks the Spanish ministry of Education for her FPU grant. Facilities provided by the Galician Supercomputing Centre (CESGA) are also acknowledged.

■ REFERENCES

(1) Rogers, R. D.; Seddon, K. R. Ionic Liquids−Solvents of the Future? *Science* **2003**, *302*, 792−793.
(2) Wasserscheid, P.; Welton, T. *Ionic Liquids in Synthesis*; Wiley Online Library: Weinheim, Germany, 2003.
(3) Dupont, J.; de Souza, R. F.; Suarez, P. A. Z. Ionic Liquid (Molten Salt) Phase Organometallic Catalysis. *Chem. Rev.* **2002**, *102*, 3667−3692.
(4) Rogers, R. D.; Seddon, K. R. *Ionic Liquids: Industrial Applications for Green Chemistry*; American Chemical Society: Washington, DC, 2002.
(5) Rogers, R. D.; Seddon, K. R. *Ionic Liquids as Green Solvents: Progress and Prospects*; American Chemical Society: Washington, DC, 2003.
(6) Earle, M. J.; Seddon, K. R. Ionic Liquids. Green Solvents for the Future. *Pure Appl. Chem.* **2000**, *72*, 1391−1398.
(7) Welton, T. Room-Temperature Ionic Liquids. Solvents for Synthesis and Catalysis. *Chem. Rev.* **1999**, *99*, 2071−2084.
(8) Anderson, J. L.; Armstrong, D. W.; Wei, G. T. Ionic Liquids in Analytical Chemistry. *Anal. Chem.* **2006**, *78*, 2892−2902.
(9) Han, X.; Armstrong, D. W. Ionic Liquids in Separations. *Acc. Chem. Res.* **2007**, *40*, 1079−1086.
(10) Garcia, B.; Lavallée, S.; Perron, G.; Michot, C.; Armand, M. Room Temperature Molten Salts as Lithium Battery Electrolyte. *Electrochim. Acta* **2004**, *49*, 4583−4588.
(11) Diaw, M.; Chagnes, A.; Carré, B.; Willmann, P.; Lemordant, D. Mixed Ionic Liquid as Electrolyte for Lithium Batteries. *J. Power Sources* **2005**, *146*, 682−684.
(12) Zhou, Q.; Henderson, W. A.; Appetecchi, G. B.; Passerini, S. Phase Behavior and Thermal Properties of Ternary Ionic Liquid−Lithium Salt (IL−IL−LiX) Electrolytes. *J. Phys. Chem. C* **2010**, *114*, 6201−6204.
(13) Lee, S. Y.; Yong, H. H.; Lee, Y. J.; Kim, S. K.; Ahn, S. Two-Cation Competition in Ionic-Liquid-Modified Electrolytes for Lithium Ion Batteries. *Green Chem.* **2005**, *109*, 13663−13667.
(14) Markevich, E.; Baranchugov, V.; Aurbach, D. On the Possibility of Using Ionic Liquids as Electrolyte Solutions for Rechargeable 5 V Li Ion Batteries. *Electrochem. Commun.* **2006**, *8*, 1331−1334.
(15) Castriota, M.; Caruso, T.; Agostino, R. G.; Cazzanelli, E.; Henderson, W. A.; Passerini, S. Raman Investigation of the Ionic Liquid *N*-Methyl-*N*-propylpyrrolidinium Bis(trifluoromethanesulfonyl)imide and Its Mixture with $LiN(SO_2CF_3)_2$. *J. Phys. Chem. A* **2005**, *109*, 92−96.

(16) Borgel, V.; Markevich, E.; Aurbach, D.; Semrau, G.; Schmidt, M. On the Application of Ionic Liquids for Rechargeable Li Batteries: High Voltage Systems. *J. Power Sources* **2009**, *189*, 331−336.
(17) Nicolau, B. G.; Sturlaugson, A.; Fruchey, K.; Ribeiro, M. C. C.; Fayer, M. D. Room Temperature Ionic Liquid−Lithium Salt Mixtures: Optical Kerr Effect Dynamical Measurements. *J. Phys. Chem. B* **2010**, *114*, 8350−8356.
(18) Nicotera, I.; Oliviero, C.; Henderson, W. A.; Appetecchi, G. B.; Passerini, S. NMR Investigation of Ionic Liquid−LiX Mixtures: Pyrrolidinium Cations and TFSI-Anions. *J. Phys. Chem. B* **2005**, *109*, 22814−22819.
(19) Lassègues, J.; Grondin, J.; Talaga, D. Lithium Solvation in Bis(trifluoromethanesulfonyl)imide-Based Ionic Liquids. *Phys. Chem. Chem. Phys.* **2006**, *8*, 5629−5632.
(20) Lassègues, J.; Grondin, J.; Aupetit, C.; Johansson, P. Spectroscopic Identification of the Lithium Ion Transporting Species in LiTFSI-Doped Ionic Liquids. *J. Phys. Chem. A* **2009**, *113*, 305−314.
(21) Egashira, M.; Todo, H.; Yoshimoto, N.; Morita, M.; Yamaki, J. Functionalized Imidazolium Ionic Liquids as Electrolyte Components of Lithium Batteries. *J. Power Sources* **2007**, *174*, 560−564.
(22) Henderson, W. A.; Passerini, S. Phase Behavior of Ionic Liquid−LiX Mixtures: Pyrrolidinium Cations and TFSI-Anions. *Chem. Mater.* **2004**, *16*, 2881−2885.
(23) Zhou, Q.; Fitzgerald, K.; Boyle, P. D.; Henderson, W. A. Phase Behavior and Crystalline Phases of Ionic Liquid-Lithium Salt Mixtures with 1-Alkyl-3-methylimidazolium Salts. *Chem. Mater.* **2010**, *22*, 1203−1208.
(24) Xu, J.; Yang, J.; NuLi, Y.; Wang, J.; Zhang, Z. Additive-Containing Ionic Liquid Electrolytes for Secondary Lithium Battery. *J. Power Sources* **2006**, *160*, 621−626.
(25) Seki, S.; Kobayashi, Y.; Miyashiro, H.; Ohno, Y.; Usami, A.; Mita, Y.; Kihira, N.; Watanabe, M.; Terada, N. Lithium Secondary Batteries Using Modified-Imidazolium Room-Temperature Ionic Liquid. *J. Phys. Chem. B* **2006**, *110*, 10228−10230.
(26) Saito, Y.; Umecky, T.; Niwa, J.; Sakai, T.; Maeda, S. Existing Condition and Migration Property of Ions in Lithium Electrolytes with Ionic Liquid Solvent. *J. Phys. Chem. B* **2007**, *111*, 11794−11802.
(27) Sakaebe, H.; Matsumoto, H. *N*-Methyl-*N*-propylpiperidinium bis(trifluoromethanesulfonyl)imide (PP13-TFSI) - Novel Electrolyte Base for Li Battery. *Electrochem. Commun.* **2003**, *5*, 594−598.
(28) Holbrey, J. D.; Seddon, K. R. Ionic Liquids. *Clean Prod. Processes* **1999**, *1*, 223−236.
(29) Rosol, Z. P.; German, N. J.; Gross, S. M. Solubility, Ionic Conductivity and Viscosity of Lithium Salts in Room Temperature Ionic Liquids. *Green Chem.* **2009**, *11*, 1453−1457.
(30) Pereiro, A. B.; Araújo, J. M. M.; Oliveira, F. S.; Esperança, J. M. S. S.; Lopes, J. N. C.; Marrucho, I. M.; Rebelo, L. P. N. Solubility of Inorganic Salts in Pure Ionic Liquids. *J. Chem. Thermodyn.* **2012**, *55*, 29−36.
(31) Zhou, Q.; Boyle, P. D.; Malpezzi, L.; Mele, A.; Shin, J.-H.; Passerini, S.; Henderson, W. A. Phase Behavior of Ionic Liquid−LiX Mixtures: Pyrrolidinium Cations and TFSI Anions — Linking Structure to Transport Properties. *Chem. Mater.* **2011**, *23*, 4331−4337.
(32) Burba, C. M.; Rocher, N. M.; Frech, R.; Powell, D. R. Cation−Anion Interactions in 1-Ethyl-3-methylimidazolium Trifluoromethanesulfonate-Based Ionic Liquid Electrolytes. *J. Phys. Chem. B* **2008**, *112*, 2991−2995.
(33) Hayamizu, K.; Aihara, Y.; Nakagawa, H.; Nukuda, T. Ionic Conduction and Ion Diffusion in Binary Room-Temperature Ionic Liquids Composed of [emim][BF4] and LiBF4. *J. Phys. Chem. B* **2004**, *108*, 19527−19532.
(34) Duluard, S.; Grondin, J.; Bruneel, J.; Pianet, I.; Grélard, A.; Campet, G.; Delville, M.; Lassègues, J. Lithium Solvation and Diffusion in the 1-Butyl-3-methylimidazolium Bis(trifluoromethanesulfonyl)imide Ionic Liquid. *J. Raman Spectrosc.* **2008**, *39*, 627−632.
(35) Umebayashi, Y.; Mitsugi, T.; Fukuda, S.; Fujimori, T.; Fujii, K.; Kanzaki, R.; Takeuchi, M.; Ishiguro, S. Lithium Ion Solvation in Room-Temperature Ionic Liquids Involving Bis(trifluoromethanesulfonyl) Imide Anion Studied by Raman Spectroscopy and DFT Calculations. *J. Phys. Chem. B* **2007**, *111*, 13028−13032.
(36) Monteiro, M. J.; Bazito, F. F. C.; Siqueira, L. J. A.; Ribeiro, M. C. C.; Torresi, R. M. Transport Coefficients, Raman Spectroscopy, and Computer Simulation of Lithium Salt Solutions in an Ionic Liquid. *J. Phys. Chem. B* **2008**, *112*, 2102−2109.
(37) Borodin, O.; Smith, G. D.; Henderson, W. Li^+ Cation Environment, Transport, and Mechanical Properties of the LiTFSI Doped *N*-Methyl-*N*-alkylpyrrolidinium$^+$TFSI$^-$ Ionic Liquids. *J. Phys. Chem. B* **2006**, *110*, 16879−16886.
(38) Niu, S.; Cao, Z.; Li, S.; Yan, T. Structure and Transport Properties of the LiPF6 Doped 1-Ethyl-2,3-dimethyl-imidazolium Hexafluorophosphate Ionic Liquids: A Molecular Dynamics Study. *J. Phys. Chem. B* **2010**, *114*, 877−881.
(39) Spoel, D. V. D.; Lindahl, E.; Hess, B.; Buuren, A. R. V.; Apol, E.; Meulenhoff, P. J.; Tieleman, D. P.; Sijbers, A. L. T. M.; Feenstra, K. A.; Drunen, R. V.; et al. *Gromacs User Manual*, version 4.0; 2005. http://www.Gromacs.org.
(40) Jorgensen, W. L. Optimized Intermolecular Potential Functions for Liquid Alcohols. *J. Phys. Chem.* **1986**, *90*, 1276−1284.
(41) Sambasivarao, S. . V.; Acevedo, O. Development of OPLS-AA Force Field Parameters for 68 Unique Ionic Liquids. *J. Chem. Theory Comput.* **2009**, *5*, 1038−1050.
(42) Prado, C. E. R.; Freitas, L. C. G. Molecular Dynamics Simulation of the Room-Temperature Ionic Liquid 1-Butyl-3-methylimidazolium Tetrafluoroborate. *J. Mol. Struct. (THEOCHEM)* **2007**, *847*, 93−100.
(43) Canongia-Lopes, J. N.; Pádua, A. A. H. Molecular Force Field for Ionic Liquids Composed of Triflate or Bistriflylimide Anions. *J. Phys. Chem. B* **2004**, *108*, 16893−16898.
(44) Darden, T.; York, D.; Pedersen, L. Particle Mesh Ewald: An *N* log(*N*) Method for Ewald Sums in Large Systems. *J. Chem. Phys.* **1993**, *98*, 10089−10094.
(45) Hess, B.; Bekker, H.; Berendsen, H. J. C.; Fraaije, J. G. E. M. LINCS: A Linear Constraint Solver for Molecular Simulations. *J. Comput. Chem.* **1997**, *18*, 1463−1472.
(46) Hess, B. P-LINCS: A Parallel Linear Constraint Solver for Molecular Simulation. *J. Chem. Theory Comput.* **2007**, *4*, 116−122.
(47) Bussi, G.; Donadio, D.; Parrinello, M. Canonical Sampling through Velocity Rescaling. *J. Chem. Phys.* **2007**, *126*, 014101.
(48) Parrinello, M.; Rahman, A. Polymorphic Transitions in Single Crystals: A New Molecular Dynamics Method. *J. Appl. Phys.* **1981**, *52*, 7182−7190.
(49) Rilo, E.; Pico, J.; Garca-Garabal, S.; Varela, L. M.; Cabeza, O. Density and Surface Tension in Binary Mixtures of CnMIM-BF4 Ionic Liquids with Water and Ethanol. *Fluid Phase Equilib.* **2009**, *285*, 83−89.
(50) Pereiro, A. B.; Legido, J. L.; Rodríguez, A. Physical Properties of Ionic Liquids Based on 1-Alkyl-3-methylimidazolium Cation and Hexafluorophosphate as Anion and Temperature Dependence. *Chem. Thermodyn.* **2007**, *39*, 1168−1175.
(51) Xuan, X.; Wang, J.; Wang, H. Theoretical Insights into PF_6^- and Its Alkali Metal Ion Pairs: Geometries and Vibrational Frequencies. *Electrochim. Acta* **2005**, *50*, 4196−4201.
(52) Francisco, J. S.; Williams, I. H. Structural and Spectral Consequences of Ion Pairing. 4. Theoretical Study of $BF_4^-M^+$ (M = Li, Na, K, and Rb). *J. Am. Chem. Soc.* **1990**, *94*, 8522−8529.
(53) Bahe, L. W. Structure in Concentrated Solutions of Electrolytes. Field-Dielectric-Gradient Forces and Energies. *J. Phys. Chem.* **1972**, *76*, 1062−1071.
(54) Varela, L. M.; Garcia, M.; Sarmiento, F.; Attwood, D.; Mosquera, V. Pseudolattice Theory of Strong Electrolyte Solutions. *J. Chem. Phys.* **1997**, *107*, 6415−6419.
(55) Varela, L. M.; Carrete, J.; Garca, M.; Rodríguez, J. R.; Gallego, L. J.; Turmine, M.; Cabeza, O. In *Ionic Liquids: Theory, Properties, New Approaches*; Kokorin, A., Ed.; InTech: New York, 2011.
(56) Arnaud, R.; Benrabah, D.; Sanchez, J.-Y. Theoretical Study of CF_3SO_3Li, $(CF_3SO_2)_2NLi$, and $(CF_3SO_2)_2CHLi$ Ion Pairs. *J. Phys. Chem.* **1996**, *100*, 10882−10891.

(57) Gejji, S. P.; Suresh, C. H.; Babu, K.; Gadre, S. R. Ab Initio Structure and Vibrational Frequencies of $(CF_3SO_2)_2N^-Li^+$ Ion Pairs. *J. Phys. Chem. A* **1999**, *103*, 7474−7480.
(58) Zhang, Y.; Alonso, P. R.; Martinez-Limia, A.; Scanlon, L. G.; Balbuena, P. B. Crystalline Structure and Lithium-Ion Channel Formation in Self-Assembled Di-lithium Phthalocyanine: Theory and Experiments. *J. Phys. Chem. B* **2004**, *108*, 4659−4668.
(59) Kowsari, M. H.; Alavi, S.; Ashrafizaadeh, M.; Najafi, B. Molecular Dynamics Simulation of Imidazolium-Based Ionic Liquids. I. Dynamics and Diffusion Coefficient. *J. Chem. Phys.* **2008**, *129*, 224508.
(60) Rey-Castro, C.; Tormo, A. L.; Vega, L. F. Effect of the Flexibility and the Anion in the Structural and Transport Properties of Ethyl-Methyl-Imidazolium Ionic Liquids. *Fluid Phase Equilib.* **2007**, *256*, 62−69.
(61) Cadena, C.; Zhao, Q.; Snurr, R.; Maginn, E. J. Molecular Modeling and Experimental Studies of the Thermodynamic and Transport Properties of Pyridinium-Based Ionic Liquids. *J. Phys. Chem. B* **2006**, *110*, 2821−2832.
(62) Qian, J.; Hentschke, R.; Heuer, A. Dynamic Heterogeneities of Translational and Rotational Motion of a Molecular Glass Former from Computer Simulations. *J. Chem. Phys.* **1999**, *110*, 4514−4522.
(63) Pópolo, M. G. D.; Voth, G. A. On the Structure and Dynamics of Ionic Liquids. *J. Phys. Chem. B* **2004**, *108*, 1744−1752.
(64) Einstein, A. Concerning an Heuristic Point of View toward the Emission and Transformation of Light. *Ann. Phys.* **1905**, *17*, 549−560.
(65) Frenkel, D.; Smit, B. *Understanding Molecular Simulation: From Algorithms to Applications*; Academic Press: New York, 1996.
(66) Liu, Z.; Chen, T.; Bell, A.; Smit, B. Improved United-Atom Force Field for 1-Alkyl-3-methylimidazolium Chloride. *J. Phys. Chem. B* **2010**, *114*, 4572−4582.
(67) Tokuda, H.; Hayamizu, K.; Ishii, K.; Susan, M. A. B. H.; Watanabe, M. Physicochemical Properties and Structures of Room Temperature Ionic Liquids. 1. Variation of Anionic Species. *J. Phys. Chem. B* **2004**, *108*, 16593−16600.
(68) Jin, H.; O'Hare, B.; Dong, J.; Arzhantsev, S.; Baker, G. A.; Wishart, J. F.; Benesi, A. J.; Maroncelli, M. Physical Properties of Ionic Liquids Consisting of the 1-Butyl-3-methylimidazolium Cation with Various Anions and the Bis(trifluoromethylsulfonyl) Imide Anion with Various Cations. *J. Phys. Chem. B* **2008**, *112*, 81−92.
(69) Borodin, O. Polarizable Force Field Development and Molecular Dynamics Simulations of Ionic Liquids. *J. Phys. Chem. B* **2009**, *113*, 11463−11478.
(70) Borodin, O. Molecular Dynamics Simulations of Ionic Liquids: Influence of Polarization on IL Structure and Ion Transport. *Mater. Res. Soc. Symp. Proc.* **2008**, *1082*, Q06−04.
(71) Tokuda, H.; Hayamizu, K.; Ishii, K.; Susan, M. A. B. H.; Watanabe, M. Physicochemical Properties and Structures of Room Temperature Ionic Liquids. 2. Variation of Alkyl Chain Length in Imidazolium Cation. *J. Phys. Chem. B* **2005**, *109*, 6103−6110.
(72) Tokuda, H.; Ishii, K.; Susan, M. A. B. H.; Tsuzuki, S.; Hayamizu, K.; Watanabe, M. Physicochemical Properties and Structures of Room-Temperature Ionic Liquids. 3. Variation of Cationic Structures. *J. Phys. Chem. B* **2006**, *110*, 2533−2839.
(73) Vila, J.; Rilo, E.; Segade, L.; Cabeza; Varela, L. M. Electrical Conductivity of Aqueous Solutions of Aluminum Salts. *Phys. Rev. E* **2005**, *71*, 031201.
(74) Angell, C. A.; Byrne, N.; Belieres, J.-P. Parallel Developments in Aprotic and Protic Ionic Liquids: Physical Chemistry and Applications. *Acc. Chem. Res.* **2007**, *40*, 1228−1236.
(75) Méndez-Morales, T.; Carrete, J.; Cabeza, O.; Gallego, L. J.; Varela, L. M. Molecular Dynamics Simulation of the Structure and Dynamics of Water−1-Alkyl-3-Methylimidazolium Ionic Liquid Mixtures. *J. Phys. Chem. B* **2011**, *115*, 6995−7008.
(76) Méndez-Morales, T.; Carrete, J.; García, M.; Cabeza, O.; Gallego, L. J.; Varela, L. M. Dynamical Properties of Alcohol + 1-Hexyl-3-methylimidazolium Ionic Liquid Mixtures: A Computer Simulation Study. *J. Phys. Chem. B* **2011**, *115*, 15322−15322.
(77) Borodin, O.; Smith, G. D.; Fan, P. Molecular Dynamics Simulations of Lithium Alkyl Carbonates. *J. Phys. Chem. B* **2006**, *110*, 22773−22779.
(78) Kowsari, M. H.; Alavi, S.; Ashrafizaadeh, M.; Najafi, B. Molecular Dynamics Simulation of Imidazolium-Based Ionic Liquids. II. Transport Coefficients. *J. Chem. Phys.* **2009**, *130*, 014703.
(79) Hansen, J. P.; McDonald, I. R. *Theory of Simple Liquids*; Academic Press: Oxford, U.K., 1986.
(80) Rey-Castro, C.; Vega, L. F. Transport Properties of the Ionic Liquid 1-Ethyl-3-methylimidazolium Chloride from Equilibrium Molecular Dynamics Simulation. The Effect of Temperature. *J. Phys. Chem. B* **2006**, *110*, 14426−14435.
(81) Rilo, E.; Vila, J.; García, M.; Varela, L. M.; Cabeza, O. Viscosity and Electrical Conductivity of Binary Mixtures of CnMIM-BF_4 with Ethanol at 288 K, 298 K, 308 K, and 318 K. *J. Chem. Eng. Data* **2010**, *55*, 5156−5163.
(82) Carda-Broch, S.; Berthod, A.; Armstrong, D. W. Solvent Properties of the 1-Butyl-3-methylimidazolium Hexafluorophosphate Ionic Liquid. *Anal. Bioanal. Chem.* **2003**, *375*, 191−199.